

# INFLUENCE OF THE FEEDSTOCK CHARACTERISTICS ON THE MICROSTRUCTURE AND PROPERTIES OF $\text{Al}_2\text{O}_3$ - $\text{TiO}_2$ PLASMA-SPRAYED COATINGS

M. Vicent<sup>1</sup>, E. Bannier<sup>1</sup>, R. Benavente<sup>2</sup>, M.D. Salvador<sup>2</sup>, T. Molina<sup>3</sup>, R. Moreno<sup>3</sup>, E. Sánchez<sup>1</sup>

(1) Instituto de Tecnología Cerámica (ITC) - Asociación de Investigación de las Industrias Cerámicas (AICE). Universitat Jaume I (UJI). Av. Vicent Sos Baynat s/n, 12006 Castellón, Spain.

(2) Instituto de Tecnología de Materiales (ITM). Universidad Politécnica de Valencia (UPV). Camino de Vera s/n, 46022 Valencia, Spain.

(3) Instituto de Cerámica y Vidrio (ICV). CSIC. c/ Kelsen 5, 28049 Madrid, Spain.

## Abstract

Atmospheric plasma spraying (APS) is an interesting technique to obtain nanostructured coatings due to its versatility, simplicity and relatively low cost. However, nanometric powders can not be fed into the plume using conventional feeding systems, due to their low mass and poor flowability, and must be adequately reconstituted into sprayable micrometric agglomerates.

In this work,  $\text{Al}_2\text{O}_3$ -13wt% $\text{TiO}_2$  nanostructured and submicron-nanostructured powders were deposited using APS. The feedstocks were obtained by spray drying from two starting suspensions, prepared by mixing two commercial nanosuspensions of  $\text{Al}_2\text{O}_3$  and  $\text{TiO}_2$ , or by adding nanosized  $\text{TiO}_2$  and submicron-sized  $\text{Al}_2\text{O}_3$  powders to water. The spray-dried granules were heat-treated to reduce their porosity and the resultant powders were fully characterised.

Optimisation of the deposition conditions enabled the reconstituted powders to be successfully deposited, yielding coatings that were well bonded to the substrate. The coating microstructure, characterised by SEM, was formed by semi-molten feedstock agglomerates surrounded by fully molten particles that act as a binder.

Moreover, microhardness, adhesion, and tribological behaviour were determined, and the impact of the granule characteristics on these properties was studied. It was found that changing the feedstock characteristics allows to control the coating quality and properties.

# 1 Introduction

Atmospheric plasma spraying (APS) is a thermal spray technique broadly used to obtain industrial coatings. This method allows the deposition of nanostructured layers with better properties than their conventional counterparts [1-5]. Still, the nanoparticles need to be previously agglomerated into a sprayable powder, as they can not be directly fed into the plasma torch [6-8]. This agglomeration process is usually done by using spray-drying [6-11] or freeze-drying [11] from a nanoparticle suspension, frequently followed by a thermal treatment in order to decrease the granule porosity [6,8]. The quality of the feedstock depends on the characteristics of the initial nanosuspension, which should present high solid content, low viscosity and high stability. However, the dispersion of nanoparticles in water to obtain such stable suspensions is an arduous task, and requires a full rheological study [9-10].

Plasma sprayed alumina-based coatings are used in a variety of applications to provide electrical insulation, increased wear resistance, and chemically unreactive surfaces [12].  $\text{Al}_2\text{O}_3\text{-TiO}_2$  coatings deposited from nanopowders have shown very promising bonding strength and wear resistance compared with conventional feedstock [13]. Moreover, the  $\text{Al}_2\text{O}_3\text{-TiO}_2$  with a 13 wt% of  $\text{TiO}_2$  displayed the best wear resistance among all the nanostructured  $\text{Al}_2\text{O}_3\text{-TiO}_2$  coatings [14].

Although many research efforts has been dedicated to scale down from the micro-scale to the nano- or submicron-scale using both powders or liquids as feedstock [1], very few studies deals with the deposition of feedstocks made by a mixture of different particle size, e.g. submicron-nano sized particles. In previous publication, it was found that the nanostructured spray-dried feedstock obtained from concentrated  $\text{Al}_2\text{O}_3\text{-13 wt% TiO}_2$  suspensions yielded coatings with lower void content than those obtained using powders from more diluted suspensions [8]. However, this study did not consider feedstocks with a bimodal particle size distribution (mixture of submicronic and nanometric particles), which are addressed in the present work.

In this paper,  $\text{Al}_2\text{O}_3\text{-13 wt% TiO}_2$  coatings were obtained by APS using commercial powders (micrometric and nanostructured) and spray-dried feedstocks. The study deals with the

relationship between the granule characteristics and coatings properties. All feedstocks were completely characterized (FEG-ESEM, granule size distribution, flowability, apparent density) and the main properties of the coatings were determined (microstructure, microhardness, toughness, wear and adhesion).

## **2 Materials and methods**

### **2.1 Feedstock preparation**

Two nanopowder suspensions of alumina and titania (VP Disp. W630X and AERODISP<sup>®</sup> W740X respectively, Degussa-Evonik, Germany), a submicron-sized powder of alumina (Condea-Ceralox HPA-0.5, Sasol, USA) and a nanopowder of titania (AEROXIDE<sup>®</sup> P25, Degussa-Evonik, Germany) were used as raw materials.

First, a 10 vol.% of 87 wt% Al<sub>2</sub>O<sub>3</sub>–13 wt% TiO<sub>2</sub> nanosuspension was prepared by mixing both commercial suspensions [8]. Secondly, a 30 vol.% of Al<sub>2</sub>O<sub>3</sub>–13 wt% TiO<sub>2</sub> submicron-nano suspension was prepared by dispersing nanosized titania particles and submicronic alumina particles in water. A commercial polyacrylic acid-based polyelectrolyte (DURAMAX<sup>™</sup> D-3005, Rohm & Haas, USA) was used as deflocculant [10,16].

In both cases, stable, well-dispersed and low-viscosity suspensions were obtained. Both suspensions were then reconstituted into sprayable granules in 2 steps:

- a) Spray-drying. Spray-dried agglomerates were obtained in a spray dryer (Mobile Minor, Gea Niro, Denmark) [8,10,11].
- b) Thermal treatments. In order to obtain denser granules, the spray-dried powders were heat treated in an electric kiln with soaking time of 60 minutes, at 1250 °C for the powder obtained from nanoparticles suspension (feedstock N) [8], and at 1200 °C for the powder obtained from the submicron-nano sized particles suspension (feedstock SN). These temperatures were chosen to obtain denser granules but at the same time to preserve as much as possible the nanostructure of the initial agglomerates.

Finally, and for comparison purposes, two commercial feedstocks with the same  $\text{Al}_2\text{O}_3\text{-TiO}_2$  weight ratio, were also deposited: a conventional microstructured one (referred as CM) and a nanostructured one (referred as CN).

All feedstock references are detailed in table I.

## **2.2 Feedstock characterisation techniques**

A field-emission gun environmental scanning electron microscope, FEG-ESEM (QUANTA 200FEG, FEI Company, USA) was used to examine the feedstock microstructure. Moreover, granule size distribution was measured by laser light scattering (Mastersizer S, Malvern, UK). Finally, powder flowability was evaluated in terms of the Hausner ratio, defined as the ratio of the tapped density to the apparent (or poured) density of the powder, and agglomerate apparent density was calculated from tapped powder density by assuming a theoretical packing factor of 0.6, which is characteristic of monosize, spherical particles [17].

## **2.3 Coating deposition**

$\text{Al}_2\text{O}_3\text{-13 wt% TiO}_2$  coatings were deposited by APS on metallic substrates (AISI 304) prepared as set out elsewhere [4]. The plasma spray system consisted of a gun (F4-MB, Sulzer Metco, Germany) operated by a robot (IRB 1400, ABB, Switzerland). The deposition was made using argon and hydrogen as plasma-forming gases. The same spraying conditions were used in all deposition experiments: Ar flow=35 slpm,  $\text{H}_2$  flow=12 slpm, arc intensity=600 A, spraying distance=0.12 m, spraying velocity=1 m/s.

## **2.4 Coating characterisation techniques**

First, the coating microstructures were observed by SEM (JSM6300, JEOL, Japan). Coating porosity was evaluated by image analysis from ten backscattered electron mode micrographs at 1000 magnification.

The hardness and fracture toughness of the materials were determined using an indentation technique. A conventional diamond pyramid indenter (Vickers) was fit to the piece of equipment (4124, INNOVATEST, Netherlands) and a load of 3 N was applied for 15 s according to the standard specification ASTM E92-72.

Wear tests were carried out under dry sliding conditions using a pin-on-disk tribometer (MT2/60/SCM/T, Microtest, Spain) in accordance with ASTM wear testing standard G99-03. As friction partner, 5 mm diameter-Si<sub>3</sub>N<sub>4</sub> ball was used. The normal load, sliding speed and distance were fixed at 10 N, 0.1 m/s and 1000 m, respectively. Testing was carried out in air, at room temperature and in dry conditions. Prior to measuring hardness, toughness and wear, the samples were polished (RotoPol-31, Struers, Denmark) with diamond to 1 μm roughness for hardness and toughness, and with SiC to 2-3 μm for wear.

The pull-off tests were performed according to ASTM D4541 in a PosiTest (AT-A, DeFelsko, USA). The dolly, whose diameter was 10 mm, was attached to the coating surface with a curable epoxy adhesive for 8 h. After that, the dolly was vertically pulled-off (with a 2.0 MPa rate) while measuring the necessary force. The results are the averages of 3 repeated tests done on each sample.

### **3 Results and discussion**

#### **3.1 Feedstock characterisation**

A former study revealed that the conventional powder (CM) is formed by angular particles between 20 and 60 μm, while the commercial nanostructured feedstock (CN) contained highly porous agglomerates of nanoparticles [4]. Moreover, both reconstituted feedstocks are made of spherical spray-dried granules composed by nanoparticles for N, and by ordered nano and mostly submicron-sized particles for SN (Figure 1). The mixing of two particles sizes in the later powder leads to a better particle packing [18] and, therefore, to a much higher agglomerate apparent density (Table II).

Figure 2 shows the granule size distribution of all feedstocks, which exhibit similar monomodal granule size distribution. It should be pointed out that the second hump observed in the curve corresponding to N powder is due to granule agglomeration during the dispersion of the powder in water. The results demonstrate that the prepared suspensions are homogeneous, even in the case of SN sample, where nano- and submicron- sized particles are randomly distributed.

The granule sizes measured by laser diffraction ( $d_{v,0.1}$ ,  $d_{v,0.5}$  and  $d_{v,0.9}$ ) are given in Table II. It was found that both commercial powders (CM and CN) displayed narrower granule size distributions and smaller granules than the reconstituted feedstocks (N and SN). In particular, both self-prepared spray-dried powders contain significantly bigger granules than the commercial spray-dried feedstock (CN).

Table II also gives the Hausner ratio and agglomerate apparent density for all the powders. On the one hand, granule apparent densities were 3800 and 2000 kg/m<sup>3</sup> for CM and CN, respectively. Indeed, CM is a fused and crushed dense powder, whereas CN is a spray-dried porous powder. On the other hand, agglomerate apparent densities of the reconstituted feedstock were 1700 kg/m<sup>3</sup> for N and 3100 kg/m<sup>3</sup> for SN, as a consequence of the better packing efficiency inside the agglomerate associated with the submicronic-nanometric particle arrangement. In terms of density, powder CN and N are quite comparable, whereas SN feedstock is more similar to the conventional powder.

Finally, the Hausner ratio for all powders was  $\leq 1.25$ , indicating good flowability and confirming that both reconstituted feedstocks are appropriate for APS process [8,10].

### **3.2 Coating microstructure**

The coatings microstructure is clearly influenced by the feedstock characteristics, as revealed by SEM observations (Figures 3 and 4). As expected, the coating obtained from the conventional powder (CM) shows a typical splat-like microstructure, formed by successive impacts of fully molten droplets. However, the layers deposited from both nanostructured powders (CN and N) exhibit a bimodal microstructure formed by partially molten agglomerates, that retained the initial nanostructure, surrounded by a fully molten matrix. Such microstructure has been reported in literature [4]. Moreover, sample SN also displayed a few partially molten areas, which are made of bigger particles than in the former case, as the feedstock mostly contained submicron particles. Yet, it has to be pointed out that these coatings are mainly formed by fully molten areas, as a consequence of the high sintering grade of the initial granules.

Differences were also found in the coating porosity as reported in table III. The coatings obtained from both commercial powders presented a lower porosity probably due to their

smaller average granule size. Indeed, smaller granules are easier to melt, giving raise to more deformable droplets, and consequently to lower coating porosity.

### **3.3 Coating mechanical properties**

Coatings mechanical properties are given in table III. The conventional layer displays the highest adhesion strength, while the other 3 coatings exhibit similar values. Such results can be explained by the morphology of the conventional feedstock, which is a dense “fused and crushed” powder instead of a porous spray-dried material. As a results of its lower porosity it should display a higher thermal conductivity [19][20], leading to an increased melting grade during deposition and thus, to a superior deformability of the droplets when they impact against the substrate, resulting in improved adhesion strength.

Moreover, nanostructured coatings (CN and N) displayed somehow lower fracture toughness than that of conventional and submicron-nanometric ones. Such results is in contradiction with the common hypothesis which suggests that the presence of partially molten nanozones can impede the propagation of cracks in nanostructured plasma-sprayed layers, since the fracture toughness of agglomerates should be higher than that of the matrix [21]. Actually, as confirmed by the SEM observations (Figure 4), the partially molten areas found in this study are highly porous, and exhibit low cohesion between the nanoparticles. As a consequence, cracks may propagate easily between the nanoparticles explaining the lower fracture toughness. This poor cohesion of the nanozones is probably due to the low density of the granules found in the corresponding feedstocks (Table II).

Furthermore, significant differences were observed in the microhardness of the coatings, which varied from 2.2 GPa, for the conventional layer, up to 9.5 GPa, for SN coating. Besides, it can be observed that, when the microhardness increases, the wear resistance of the coating is improved. In fact, the best wear performance was found for SN coating while CM layer displayed the highest wear loss. Both nanostructured coatings (CN and N) show an intermediate behaviour, with a significantly higher wear resistance than that of the conventional layer.

In spite of the existence of some correlation between microhardness and wear resistance (Figure 5), it has to be pointed out that the fracture toughness also plays a key role, as both deformation

and microfracture are usually involved in wear mechanisms. Actually, the ratio between hardness (resistance to deformation) and fracture toughness (resistance to fracture), called brittleness index (B) [22], can be used to determine the relative wear resistance of bulk materials [23]. In this study, it was found that the wear loss of the coatings decreases when their brittleness index increases, with a linear relationship between both magnitudes (Figure 5). Such results are in accordance with the study made by Boccaccini [23], which established that for low values of the brittleness index ( $B < 4 \mu\text{m}^{-1/2}$ ) the wear rate is reduced when B is increased, as in such conditions the mechanisms of material removal involve both plastic deformation and microfracture. As a consequence, it may be interesting to take into account the brittleness index, instead of hardness or fracture toughness separately, to explain the wear behaviour of thermal-sprayed coatings.

## 4 Conclusions

In this study, four different  $\text{Al}_2\text{O}_3$ -13 wt%  $\text{TiO}_2$  feedstocks have been deposited by APS: a fused and crushed conventional powder, a commercial nanostructured spray-dried powder and two reconstituted powders. Both reconstituted feedstocks were prepared by spray-drying and subsequent thermal treatment from stabilized aqueous suspension obtained, in one case, by mixing two commercial nanoparticles suspensions, and in the other case, by dispersing  $\text{TiO}_2$  nanoparticles and  $\text{Al}_2\text{O}_3$  submicron-sized particles into water.

In general, the coatings obtained from the submicron-nanometric reconstituted powder leads to better coatings properties whereas the conventional coatings display the worst wear behaviour. Both nanostructured feedstocks (commercial and self-prepared) give raise to similar properties. Finally, it should be highlighted that coating microstructure and properties are clearly influenced by the feedstocks characteristics, which demonstrates that the initial powder properties should be optimised, along with the spraying parameters, in order to obtain coatings with superior performances.



## ACKNOWLEDGEMENTS

This work has been supported by the Spanish Ministry of Science and Innovation (project MAT2009-14144-C03).

## REFERENCES

- [1] P. Fauchais, M. Vardelle, J.F. Coudert, A. Vardelle, C. Delbos, J. Fazilleau, *Pure Appl. Chem.* 77 (2005) 475-485.
- [2] R.S. Lima, B.R. Marple, *J. Therm. Spray Technol.* 16 (2007) 40-63.
- [3] L. Pawlowski, *Surf. Coat. Technol.* 202 (2008) 4318-4328.
- [4] E. Sánchez, V. Cantavella, E. Bannier, M.D. Salvador, E. Klyastkina, J. Morgiel, J. Grzonka, A. Boccaccini, *J. Therm. Spray Technol.* 17 (2008) 329-337.
- [5] A. Rico, P. Poza, J. Rodríguez, *Vacuum* (2012), doi:10.1016/j.vacuum.2012.01.008.
- [6] L.L. Shaw, D. Goberman, R. Ren, M. Gell, S. Jiang, Y. Wang, T.D. Xiao, P.R. Strutt, *Surf. Coat. Technol.* 130 (2000) 1-8.
- [7] M. Gell, E.H. Jordan, Y.H. Sohn, D. Goberman, L. Shaw, T.D. Xiao, *Surf. Coat. Technol.* 146-147 (2001) 48-54.
- [8] E. Sánchez, A. Moreno, M. Vicent, M.D. Salvador, V. Bonache, E. Klyatskina, I. Santacruz, R. Moreno, *Surf. Coat. Technol.* 205 (2010) 987-992.
- [9] S. Fazio, J. Guzmán, M.T. Colomer, A. Salomoni, R. Moreno, *J. Eur. Ceram. Soc.* 28 (2008) 2171-2176.
- [10] M. Vicent, E. Sánchez, A. Moreno, R. Moreno, *J. Eur. Ceram. Soc.* 32 (2012) 185-194.
- [11] M. Vicent, E. Sánchez, T. Molina, M.I. Nieto, R. Moreno, *J. Eur. Ceram. Soc.* 32 (2012) 1019-1028.
- [12] J.M. Guilemany, J. Nutting, M.J. Dougan, *J. Therm. Spray Technol.* 6 (1997) 425-429.
- [13] J. Ahn, B. Hwang, E.P. Song, S. Lee, N.J. Kim, *Metall. Mater. Trans. A* 37 (2006) 1851-1861.
- [14] X. Lin, Y. Zeng, S.W. Lee, C. Ding, *J. Eur. Ceram. Soc.* 24 (2004) 627-634.
- [15] G. Darut, H. Ageorges, A. Denoirjean, G. Montavon, P. Fauchais, *J. Therm. Spray Technol.* 17 (2008) 788-795.
- [16] T. Molina, M. Vicent, E. Sánchez, R. Moreno *Mater. Res. Bull.* (2012), <http://dx.doi.org/10.1016/j.materresbull.2012.05.016>.
- [17] J.L. Amorós, A. Blasco, J.E. Enrique, F. Negre, *Bol. Soc. Esp. Ceram. Vidr.* 26 (1987) 31-37.
- [18] C.C. Furnas, Bur. Mines Rep. Invest. 2894 (1928) 1-10.
- [19] Z. Zivcová, E. Gregorová, W. Pabst, D.S. Smith, A. Michot, C. Poulhier, *J. Eur. Ceram. Soc.* 29 (2009) 347-353.
- [20] C. Lee, H. Choi, C. Lee, H. Kim, *Surf. Coat. Technol.* 173 (2003) 192-200.
- [21] P. Bansal, N.P. Padture, A. Vasiliev, *Acta Mater.* 51 (2003) 2959-2970.
- [22] B.R. Lawn, D.B. Marshall, *J. Am. Ceram. Soc.* 62 (1979) 347-350.
- [23] A.R. Boccaccini, *Interceram*, 48 (1999) 176-187.

## TABLES

Table I. References and descriptions of the feedstocks used in this study

<b>Feedstock</b>	<b>Description</b>	<b>Supplier reference</b>
<b>CM</b>	<u>C</u> ommercial <u>M</u> icrometer powder	Metco 130, Sulzer Metco, Germany
<b>CN</b>	<u>C</u> ommercial <u>N</u> anostructured powder	Nanox™ S2613S, Inframat Advanced Materials, USA
<b>N</b>	Spray-dried <u>N</u> anostructured powder obtained from commercial nanosuspensions and heat-treated at 1250 °C	---
<b>SN</b>	Spray-dried <u>S</u> ubmicron- <u>N</u> anometric powder obtained from self-prepared suspensions of Al <sub>2</sub> O <sub>3</sub> submicron-sized and TiO <sub>2</sub> nanometric particles and heat-treated at 1200 °C	---

**Table II. Main characteristics of the powders (commercial ones and spray-dried granules obtained from nanosuspensions and from submicron-nano suspensions)**

Reference	Particle		Granule				
	Mean size (*) (nm)		Laser diffraction			Powder flowability	
	Al <sub>2</sub> O <sub>3</sub>	TiO <sub>2</sub>	D <sub>v, 0.1</sub> (µm)	D <sub>v, 0.5</sub> (µm)	D <sub>v, 0.9</sub> (µm)	Hausner ratio	Agglomerate apparent density (kg/m <sup>3</sup> )
<b>CM</b>	n.a.		22	36	53	1.28	3800
<b>CN</b>	50-500		17	38	66	1.19	2000
<b>N</b>	13	21	32	70	198	1.20	1700
<b>SN</b>	350	21	23	57	139	1.25	3100

(\*) Supplier data

**Table III. Coatings properties**

	<b>CM</b>	<b>CN</b>	<b>N</b>	<b>SN</b>
<b>Porosity (%)</b>	3	3	8	6
<b>Adhesion strength (MPa)</b>	10.0	7.5	7.8	7.7
<b>Vickers microhardness (GPa)</b>	2.2	4.2	5.3	9.5
<b>Fracture Toughness (MPa·m<sup>1/2</sup>)</b>	1.10	0.59	0.60	1.00
<b>Wear loss (10<sup>-10</sup>·kg/mN)</b>	1.76	0.39	0.29	0.08
<b>Brittleness Index (μm<sup>-1/2</sup>)</b>	0.0020	0.0071	0.0088	0.0095

## **FIGURE CAPTIONS**

Figure 1. FEG-ESEM micrographs, at two magnifications, of spray-dried granules after calcination

Figure 2. Granule size distributions measured by laser light scattering

Figure 3. SEM micrographs showing the general microstructure of all as-sprayed coatings, partially molten areas are referred as “pm”

Figure 4. High magnification SEM micrographs of the partially molten areas found in coatings CN, N and SN

Figure 5. Evolution of the wear loss as a function of the microhardness or of the brittleness index

## FIGURES

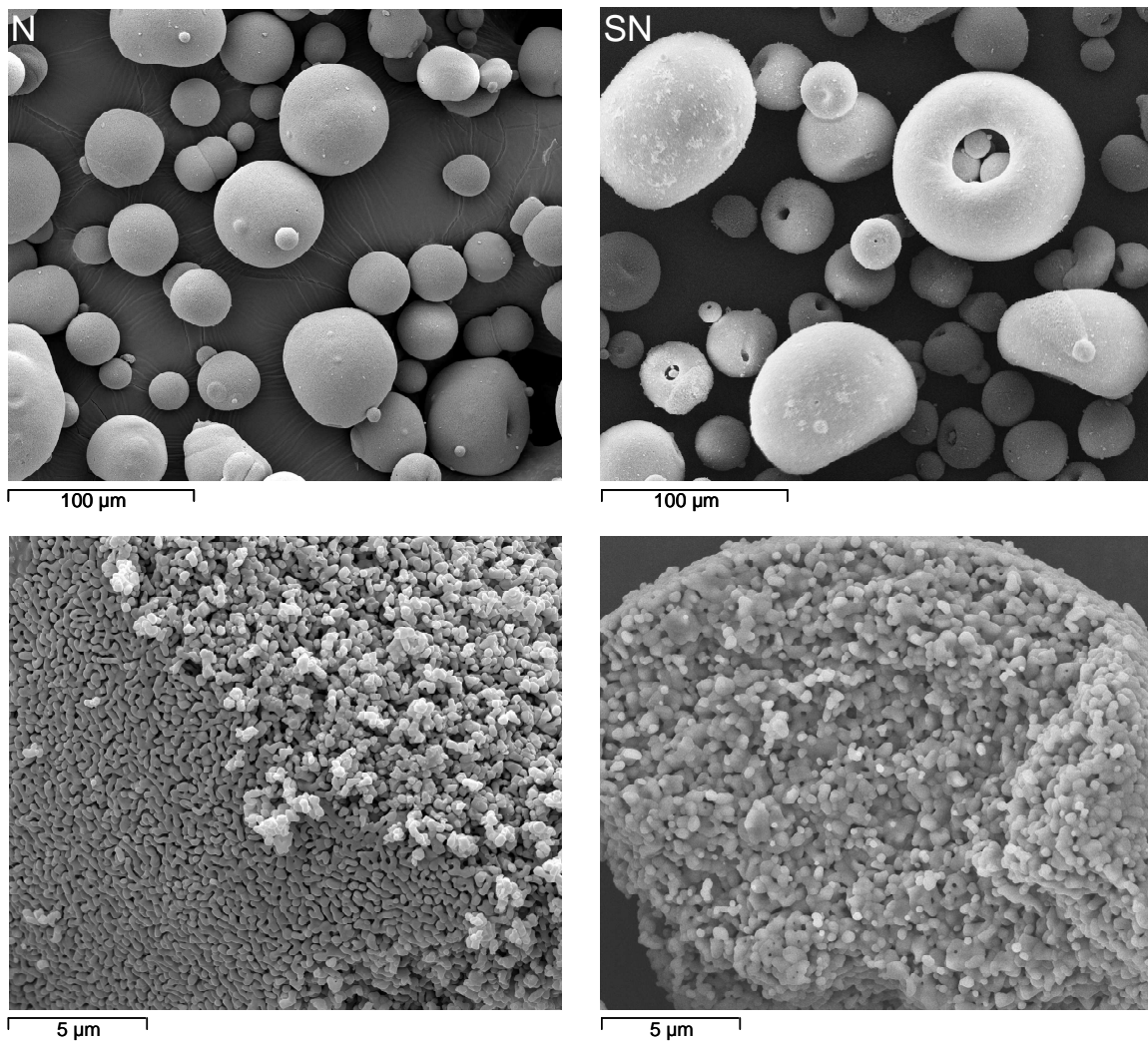


Figure 1

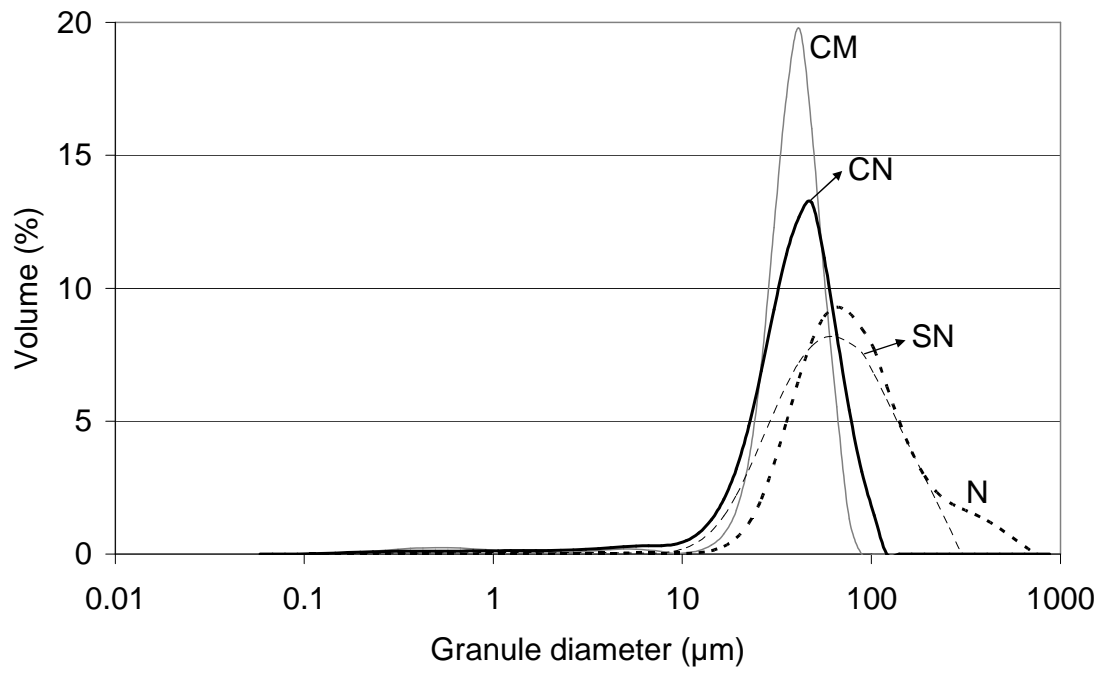
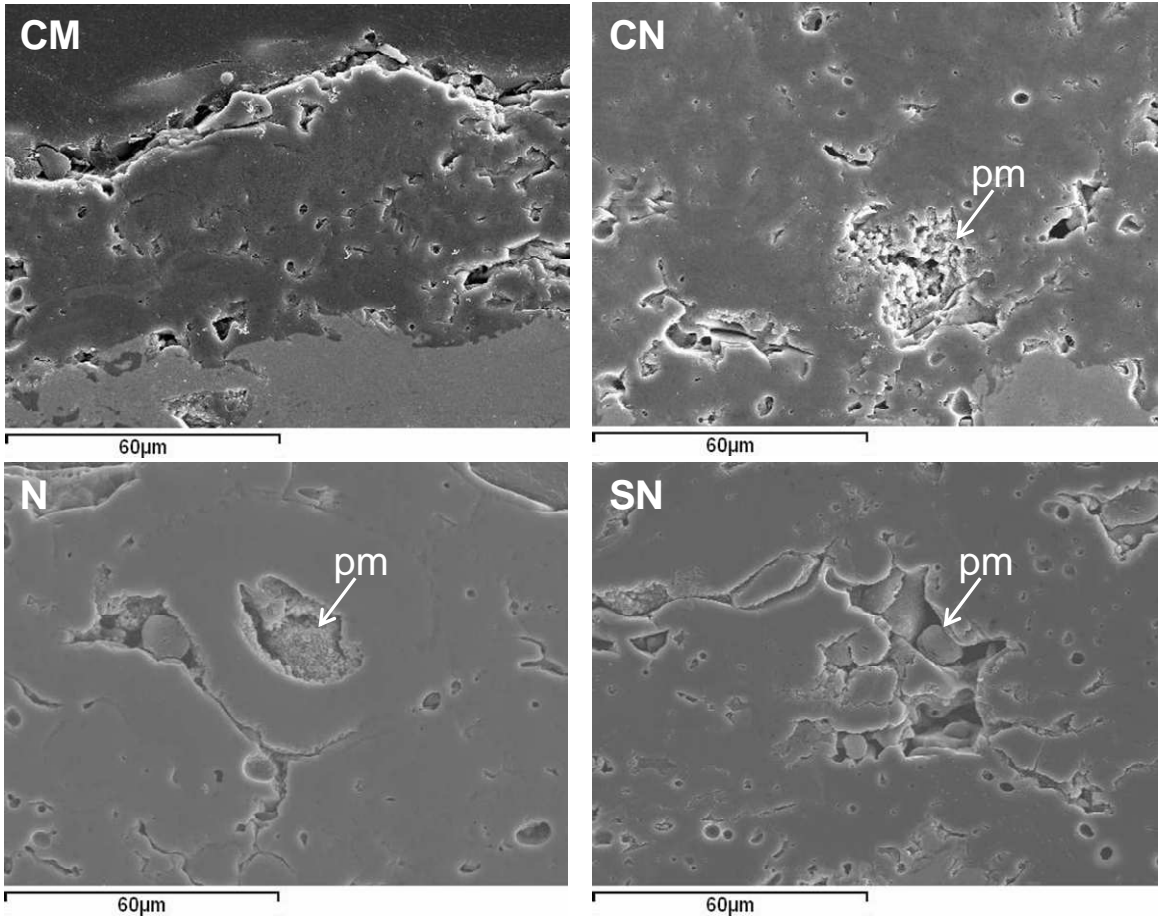
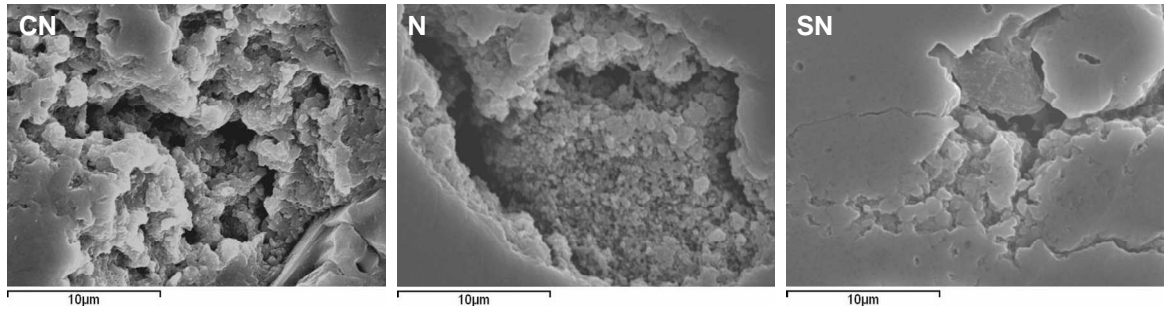


Figure 2



**Figure 3**





**Figure 4**

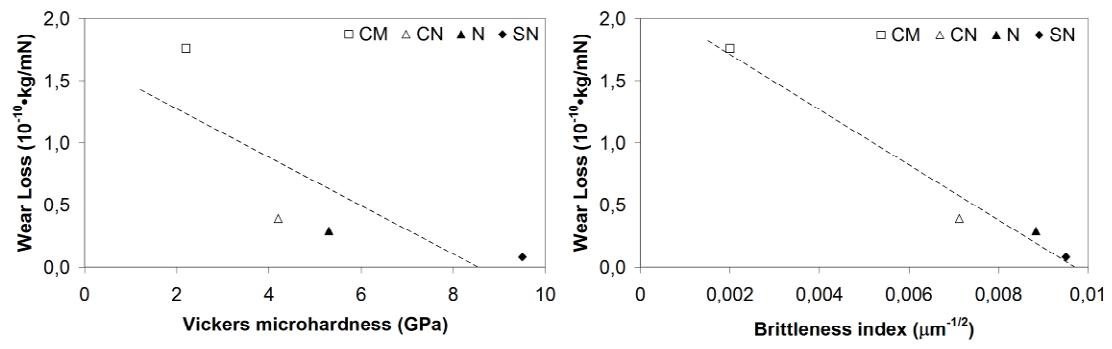


Figure 5